American Journal of Remote Sensing
2025, Vol. 13, No. 2, pp. 73-86
https://doi.org/10.11648/j.ajrs.20251302.12

Research Article

Evaluation of the Changes of Vegetation Cover Impact on Rainfall Using Remote Sensing in Wag Hemra Zone, Amhara Region, Ethiopia

Wendimnew Getachew Alemu*

Development Meteorology, Ethiopian Meteorology Institute, Kombolcha, Ethiopia

Abstract

Landsat imagery has the ability to assess the effect of vegetation cover change on rainfall. CHRIPS data was also used to analyze rainfall time series and trend line from 1990-2024. The goal of this study was to examine temporary and spatial changes in vegetation cover impact on rainfall, examine the trends of rainfall and the correlation between rainfalls with vegetation cover change during the study period. The study methods were undertaken using NDVI, change detection, Mann-Kendall's and Sen's slope test and correlation analysis. This study explores using NDVI analysis, the vegetation cover was shown 13.5% in 1990, 29.8% in 2000, 20.2% in 2010, 31.3% in 2020 and 24.1 in 2024 over the study area. Therefore, the amount of vegetation cover has been regenerated by about 89,272 hectares (10.7%) in the past 35 years in the study area. this study results, the minimum, maximum and mean rainfalls have declined trend lines of 0.497, 0.81 and 0.26mm per year over the past 35 years period (1990-2024) respectively. Statistically non-significant trends were shown in maximum and mean rainfall but not in minimum rainfall. However, the analysis of the trend line explained that the minimum, maximum, and mean rainfalls were changed by the factors of -0.497 mm, -0.81mm, and -0.26 mm per year respectively. The mean rainfall of the vegetated area was greater than the mean rainfall of non-vegetated area for all reference years. This indicates areas with low vegetation cover or low NDVI values have shown low mean rainfall. Based on the coefficient of determination, 3% of vegetation cover change was caused by rainfall in the study area. All the residents of Wag Hemra zone are to strengthen the protection of the vegetation cover in the study area and encourage afforestation work.

Keywords

Vegetation Cover, NDVI, Remote Sensing, Rainfall, Wag Hemra

1. Introduction

Controlling vegetation cover changes is important in arid and semi-arid area due to the inadequate and delicate nature of the plant cover. Due to expected changes in vegetation cover, land productivity and biodiversity might be affected [1]. Vegetation cover change can help to predict the recurrence of natural disasters, and provide humanitarian assistance [2]. The percentage of vegetation cover is also used as a parameter to estimate the annual removal of vegetation, which refers to the degradation condition in the regions spatially [3]. The transformation of different levels of vegetation cover types was

*Corresponding author: wendimnewgetachew@gmail.com (Wendimnew Getachew Alemu)

Received: 14 September 2025; **Accepted:** 11 October 2025; **Published:** 30 October 2025

characterized by the transformation from low-cover areas to high-cover areas [4]. Changes in vegetation cover can have an impact on the climate system by changing the components of an area’s climate [5]. The land-use intensification and drastic reduction in vegetative cover are considered pervasive threats to the natural environment and biodiversity, yet the rate of reduction of vegetative cover is little known globally, but it has been reported that vegetative cover and, more importantly, forest cover change are accelerating in the present time [6]. Changes in vegetation cover directly impact surface water and energy budgets through plant transpiration, surface albedo, emissivity, and roughness [7]. One of the oldest vegetation indicators used to track dryness is the Normalized Difference Vegetation Index (NDVI), which has been used since the 1980s [8, 9].

The changes in vegetation cover were the appearance of heat and cold waves, clouds, and rainfall patterns [10]. Vegetation cover has a positive impact on local rainfall [11]. The seasonal correlation between NDVI and rainfall was negative except in the winter and post-monsoon seasons, where the correlation was slightly positive in Nepal [12]. In semi-arid zones, rainfall is thought to be the most important factor influencing plant development [13]. Changes in vegetation, land use and land cover are closely correlated with changes in seasonal rainfall [14]. There was a notable association between high-class NDVI-positive regions and wet years [15]. The vegetation of drier areas was found to be more dependent on rainfall [16], and quantified the indirect effects of rainfall on vegetation growth.

The main factors contributing to deforestation and forest degradation in the area were the shifting of agriculture, logging, and the development of communities, which increased agricultural yields and altered rainfall patterns, which in turn led to an increase in pests and diseases. Due to anthropogenic factors, vegetation was being lost, which affected the local climate and rainfall factors [17]. The rainfall situations decreased due to decreased vegetation cover, due to the direct effects of low rainfall volumes resulting from the lower native vegetation cover [18]. The depletion of forest resources contributes significantly to the climatic and physical changes of the environment [19]. Remote sensing provides the spectral data from the satellites without any physical contact with the object in digital form. This digital data is converted into a visual image in the form of imagery [20]. With the introduction of remote sensing systems and image processing software, the importance of remote sensing in geospatial information systems (GIS) has expanded significantly [21].

The gap of the study vegetation cover change was lead to the increment of unseasonal and variability of rainfall, soil erosion, flooding and loss of crop production has been expected over the study area. The present study area has not been studied in Wag Hemra zone related to the effect of vegetation cover change on rainfall. The basic argument why this study was proposed and done in Amhara Regional State, Wag Hemra zone, is that it is characterized by rapid change in vegetation cover, climate, and topographic trends. The study area focused on a gap fill that the fields of conservation and rehabilitation must address, important to understand vegetation-atmosphere interactions and their effects on climate. The findings of the study were also provided information about vegetation cover change and its effect on the climate as an input for planning and decision-making is what signifies the importance of this research. Therefore, the goal of this study was to examine how the area's temporary and spatial changes in vegetation cover affect rainfall, examine the trends of rainfall and the correlation between rainfalls with vegetation cover change during the study period.

2. Materials and Method

2.1. Description of the Study Area

Wag Hemra is one of zones in Amhara Region of Ethiopia. It is bordered on the south by Wag Hemra, on the southwest by South Gondar, on the west by North Gondar, and the north and east by the Tigray Regional state (figure 1). It is located at 38 °15’ 0” to 39 °15’ 0” E longitudes to 12 °25’ 0” to 13 °25‘0” N latitudes. The elevation of the area ranges from 989 to 4043m above sea level. This study area has eight Woredas, one administrative town and 125 Kebeles.

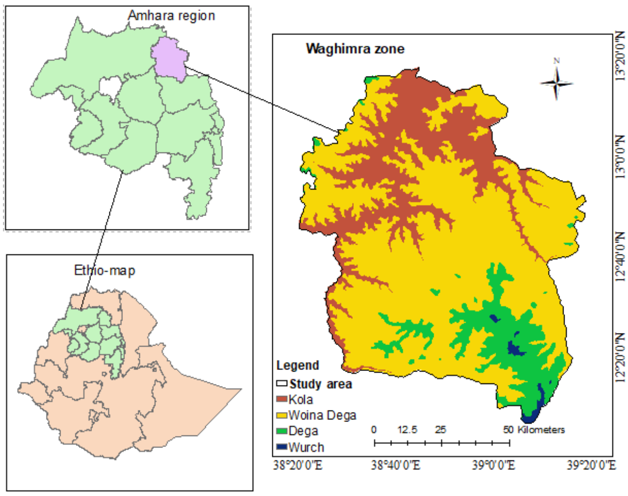

Figure 1. *Location map of study area.*

2.2. Source of Data

2.2.1. Landsat Data

The United States Geological Survey (USGS) is a gold mine of information and a source of free satellite images that cover wide areas. For this reason, both the Landsat 5 Thematic Mapper (Landsat 5TM), and Landsat-8 Operational Land Imager (OLI) were used Landsat collection two level two used 1990, 2000, 2010, 2020 and 2024 respectively, with path

169 with raw 051. Landsat 5TM and Landsat 8 OLI were used for vegetation cover change analysis to know the extent of deforestation in Wag Hemra zone for the last 35 years (1990 to 2024). All the Landsat images were included 30m spatial resolution and to analyze the effect of vegetation cover change using three decadal and half data sets. February to April months and zero percent or cloud-free images was used in this study. Because dry-season images were used to separate evergreen vegetation from rainfall-dependent vegetation likes grass and other agricultural crops. Google Earth points were used for historical data classification and exactness evaluation using the Google Earth Pro tool.

2.2.2. Rainfall Data

CHIRPS is a gridded merged satellite-station rainfall data product with a 40+ year record, quasi-global extent, and 5 km resolution [22]. CHIRPS is widely used for drought early warning, agro-climatological monitoring, and historical climate impact and trend assessments [23]. To assess the trends of rainfall, the monthly product of Climate Hazards Group Infrared Rainfall with Stations (CHIRPS) time series data from 1990 to 2024 has been used. The reason CHIRPS data were selected from other satellite-based rainfall estimation product is that the CHIRPS product corresponds best to the rain gauge values [24, 25].

Table 1. *Description of Satellite Images.*

Satellite	Spatial Resolution	Path & Row	Date of Acquisitions and Sensors				
			Landsat 5 TM			Landsat 8 OLI	
			1990	2000	2010	2020	2024
Landsat	30M	169 & 051	07/01/1990	19/01/2000	14/01/2010	26/01/2020	22/02/2024
CHRIPS	5km/month		January- April /1990-2024				

2.3. Method

2.3.1. Image Preprocessing

Satellites images are have not been directly utilized for feature identification or any other applications. Pre-processing has been applied before the main data analysis and extraction of information to reduce the number of mistakes that influence the ultimate result of the study. In this study, layer stacking and image enhancement were applied using ENVI software (Environment for Visualizing Images). To prepare a vegetation cover map of the study area, bands 1 to 7, except band 6, were stacked in the case of Landsat 5 TM, and bands 2 to 7 were stacked in the case of Landsat 8 OLI/TIRS (Thermal Infra-Red) [11]. Layer stacking of individual bands was done to get the multispectral image with all band combinations [2].

2.3.2. Normalized Difference Vegetation Index (NDVI)

The most widely used method for detecting vegetation greenness is the Normalized Difference Vegetation Index using the Landsat 5 TM and 8 OLI collection two level two [26]. The NDVI is the difference in reflectance between near-infrared and red light, which is used to evaluate the health and greenness of vegetation cover in a study area [27]. The NDVI was used assessing vegetation condition. NDVI values has been determined from the below proportions as follows [28]:

$$NDVI = \frac{NIR-R}{NIR+R} \tag{1}$$

Where NDVI = Normalized Difference Vegetation Index.

NIR = Near Infrared Band (TM and ETM band 4, OLI band 5 and band 8 for sentinel image) and.

R = Red Band (TM and ETM band 3, OLI band 4 and band 4 for sentinel image).

The NDVI was estimated from Landsat images and has characteristic values between -1 and 1. Negative NDVI indicates clouds, water, snow, and other non-vegetation cover. Values of +0.1 and more show vegetation cover. NDVI up to 0.1 indicates poor vegetation cover, which might be due to unfavorable weather conditions, whereas a high NDVI indicates dense vegetation conditions [29].

2.3.3. Change Detection

Change Detection is critically important application of remote sensing that focuses on identifying, mapping, and analyzing changes in vegetation or non-vegetation over a study period [30]. The change detection formula is provided by the following equation:

$$\text{Change difference} = \text{NDVI\_t2} - \text{NDVI\_t1} \tag{2}$$

Where t2 and t1 are the Normalized Difference Vegetation Index values at time.

2.3.4. Accuracy Assessment

Accuracy assessment is a measure of agreement between a standard assumed to be correct and a classified image of unknown quality. If the classified image corresponds closely with the standards, it is said to be accurate [31]. The accuracy of the classified image compares how each of the classified pixels with the Google earth points recorded from their corresponding ground truth data [21]. A set of reference pixels representing geographic points from Google Earth on the classified image is required for the accuracy assessment. Due to this 75 Google Earth points for each year were used to the threshold and to validate the result of 2020 and 2024 Landsat images to validate the accuracy of the result [11].

In accuracy assessment, the kappa coefficient is a basic measure that was utilized to statistically determine, in the event that the remotely detected classification is better than an irregular classification and on the off chance that two or more error matrices are altogether distinct from each other.

$$K= \frac{N\sum_{j=1}^{n} xjj-\sum_{j=1}^{n}(xj+*x+j)}{N^2-\sum_{j=1}^{n}(xj+*x+j)} \tag{3}$$

where k is kappa statistics, N is total samples, xjj is the number of rows j and columns j, xj+ is row total, and x+j is column total.

The Kappa coefficient is a frequently used method for comparing classified and actual vegetation cover. The kappa coefficient value ranges from -1 to +1; the higher the value, the greater the agreement where as a value close to zero means that the agreement is no better than would be expected by chance [31, 32]. These values fall into three branches: firstly, more prominent than 0.80 spoken to solid understanding; secondly, between 0.40 and 0.80 spoken to direct understanding; and less than 0.40 spoken to destitute understanding between the classification and reference information. The classification accuracy of remotely sensed images is widely assessed using the error matrix [33].

Finally, the following equations were used to calculate producer accuracy, user accuracy, and overall accuracy using the error matrix method in Microsoft Excel.

$$\text{PA (\%)} = \frac{NAVC}{TRVC} X\ 100 \tag{4}$$

Where PA is producer accuracy, NAVC is number of accurately identified points in an individual vegetation cover category and TRVC is total reference points of respective vegetation cover category.

$$\text{UA (\%)} = \frac{NAVC}{TCRP} \text{ x } 100 \tag{5}$$

Where UA is user accuracy and TCRP is total number of classified reference points.

$$\text{OA (\%)} = \frac{SCC}{TS} * 100 \tag{6}$$

Where OA is overall accuracy, SCC is the sum of correctly classified items, and TS is the total sample. The overall accuracy of the classified image is determined by comparing how each satellite image cell is classified to the definite land cover conditions acquired from the actual land cover [34].

2.3.5. Mann-Kendall (MK) and Sen's Slope Trend Test

The MK trend test is a non-parametric test based on two hypotheses: one is null (H0), and the other is the alternative (H1) hypothesis [35]. The MK test is based on a null hypothesis (H0), which means that there is no trend and the data are independent and randomly ordered, and this is verified against the alternative hypothesis (Ha), which supposes that there is a trend [36]. The Mann-Kendall test formula is provided by the following equation:

$$S=\sum_{i=1}^{n-1}\sum_{j=i+1}^{n} sign(yj-yi) \tag{7}$$

The trend test is applied to a time series yj, which is ranked from i = 1, 2, 3,... n – 1 and yi, which is ranked from j = i + 1, i + 2, i + 3,... n. Each of the data point's yj is taken as a reference point, which is compared with the rest of the data point's yi.

According to [37], a positive value of S means an increasing trend, and a negative value shows a decreasing trend.

$$\text{Sign (yj-yi)} = \begin{cases} +1, if\ (yj-yi) > 0 \\ 0, if\ (yj-yi) = 0 \\ -1, if\ (yj-yi) < 0 \end{cases} \tag{8}$$

Where yj and yi are the sequential data values and n is the length of the data set.

This particular test was calculated using R-studio or R-programming for Window and the XLSTAT tool.

2.3.6. Correlation Analysis

In correlated data analysis, the change in the magnitude or trends of rainfall is associated with a change in the magnitude of NDVI, and either in the positive correlation or negative correlation [38].

Correlation coefficients are scaled such that they range from -1 to +1 inclusive, where 1 is a total positive correlation, 0 is no correlation, no linear or monotonic association, and − 1 is a negative correlation [39]. The correlation coefficients of the two variables are expressed in the following equation (9):

$$Rxy = \frac{\sum_{i=1}^{n}(xi-xm)*(yi-ym)}{\sqrt{\sum_{i=1}^{n}(xi-xm)^2\sum_{i=1}^{n}(yi-ym)^2}} \tag{9}$$

Where Rxy is the simple correlation coefficient of variables x and y, xi is the NDVI or vegetation cover of the ith year or month, Yi is the rainfall of the ith year or month, Xm is the average NDVI or vegetation cover for all years or months, and Ym is the average rainfall for all years or months.

3. Results and Discussion

3.1. Detection of Normalized Difference Vegetation Index (NDVI)

The current study investigated the effect of changing the amount of vegetation on rainfall in Wag Hemra zone. In this study, NDVI was calculated from Landsat images of 1990, 2000, 2010, 2020 and 2024 to assess the extent of vegetation cover change over the study area. Many researchers used it to assess vegetation cover change and showed trends of climate variability in many areas [11, 39]. The darker green color NDVI image in the southern part of the study suggested that it had the highest NDVI values and the highest vegetation coverage. Otherwise, the red color, as shown in Figure 2, has the lowest NDVI values, which mean non-vegetation cover such as water, bare land, and roads over the study area. The study agrees with the low value of NDVI, which represents no vegetation such as water, soil, and urban areas, while green-colored areas represent high vegetation such as agriculture land, forest and vegetation [9].

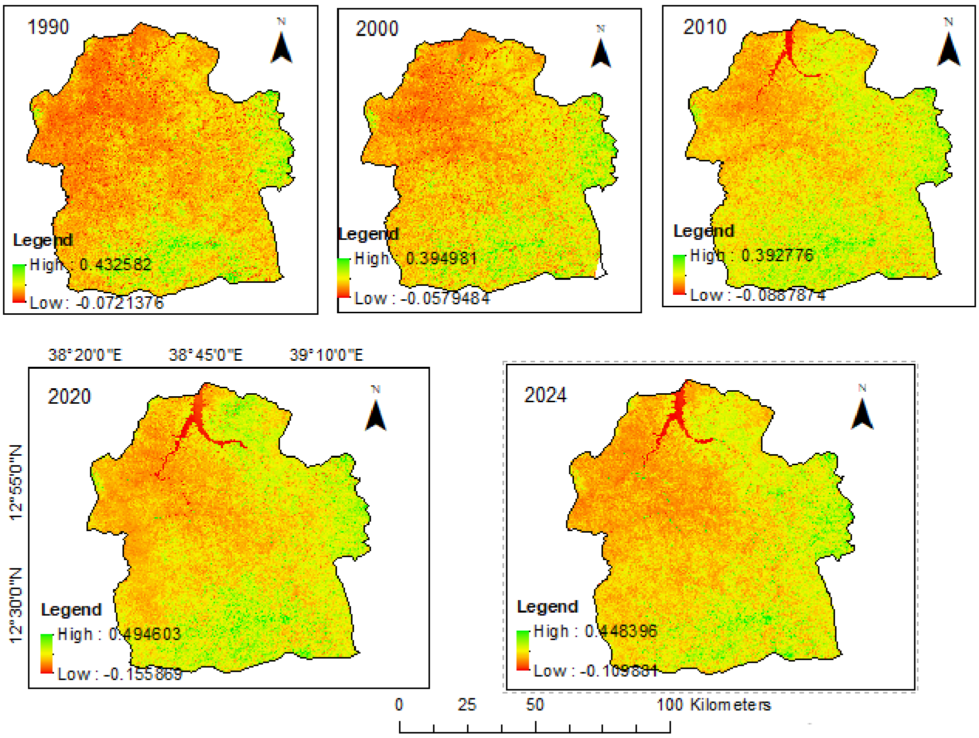

Figure 2. *NDVI map of 1990, 2000, 2010, 2020 and 2024. Sources: from Landsat satellite image.*

The minimum and maximum NDVI values of 1990 and 2000 were -0.07 to +0.433 and -0.058 to +0.395 respectively. The mean values of 1990 and 2000 were increased from +0.067 to +0.085, as shown in Table 2. This showed that higher and healthier vegetation cover was obtained in 2000. The minimum and maximum NDVI values of 2010 and 2020 were -0.089 to +0.393 and -0.156 to +0.495 respectively. The mean value was decreased to +0.078 in 2010 and increased to +0.0843 in 2020 as compared with 2000. The minimum and maximum NDVI values of 2024 were ranges -0.11 to +0.448, and its mean NDVI value was +0.0797. The highest mean NDVI value was observed in 2000 as compared to all reference years. This revealed that the status of vegetation cover improved in this year. Therefore, the mean NDVI values of all reference years were below 0.1, which means non-vegetation cover have greater area coverage than vegetation cover in the study area (1990-2024).

Table 2. *Summary of NDVI results.*

Year/parameter	1990	2000	2010	2020	2024
Minimum	-0.07	-0.058	-0.089	-0.156	-0.110
Maximum	0.433	0.395	0.393	0.495	0.448
Mean	0.067	0.085	0.078	0.0843	0.0797

Source: Computed from USGS Landsat satellite image

3.2. Vegetation and Non-Vegetation Cover Map

According to the analysis of vegetation and non-vegetation cover mapping in Figure 3, vegetation cover has been detected the green color in the eastern and southern parts of the study area for 1990, 2000, 2010, 2020 and 2024. On the other hand, the non-vegetation cover showed the orange color in the western, central and north parts of the study area. Therefore, the area of non-vegetation covers was greater than the area of vegetation cover.

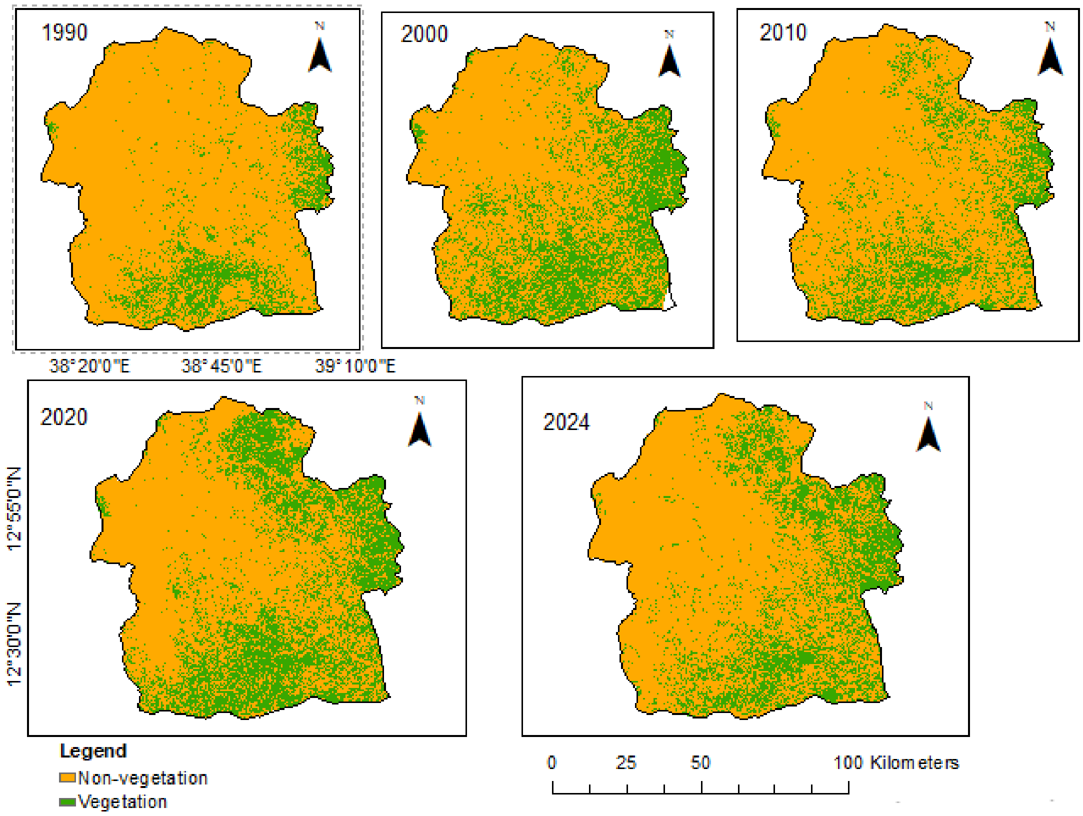

Figure 3. *Vegetation and non-vegetation cover map of 1993, 2000, 2010 and 2022.*

As indicated in Table 3, vegetation and non-vegetation covers in 1990 were 112,280 ha and 722,480 ha respectively. This suggested that the vegetation cover account for 13.5% in 1990 of the study area. The vegetation and non-vegetation covers in 2000 were 248,560 ha (29.8%) and 586,202 ha (70.2%), respectively, which means that the vegetation cover increased by 136,280 ha from reference year 1990 to 2000. The vegetation and non-vegetation cover in 2010 were 168,321 ha (20.2%) and 666,441 ha (79.8%), respectively. This indicated that the vegetation cover decreased by 80,239 ha, and this indicated vegetation cover degraded in 2010 as compared to 2000. Vegetation covers in 2020 were 261,268 ha (31.3%), which implies that the vegetation covers were expanded by 92,947 ha from 2010 to 2020. The vegetation and non-vegetation cover in 2024 were 201,552 ha (24.1%) and 633,210 ha (75.9%), which means the vegetation cover degraded in this year compared to 2020. During the analysis, the largest area of vegetation cover was expanded in 2020, which accounts for 31.3%. On the other hand, the least area of vegetation cover was exhibited during the period of 1990, which accounted for 13.5% of the study area.

Table 3. *Vegetation and non-vegetation cover showing the area in hectare for the year 1993, 2000, 2010 and 2022.*

Land cover	1990	2000	2010	2020	2024
Vegetation	112,280	248,560	168,321	261,268	201,552
Non-vegetation	722,480	586,202	666,441	573,494	633,210
Total	834,762	834,762	834,762	834,762	834,762

Source: Computed from Landsat image

3.3. Vegetation Cover Change Detection

Using image differencing (Table 4), there was the largest vegetation restored area from 1990 to 2020 at 166,598 ha and the smallest vegetation eliminated area from 1990 to 2000 at 13,363 ha. This implies that the vegetation expanded area occupied 20%, while the smallest vegetation cover changed area also occupied 1.6% of the study area. Change detection analysis of image differentiation revealed that the highest vegetation removed from the area (from vegetated to non-vegetated) between 2010 and 2020 was 190,755 ha (22.9%). From the image differentiation analysis, the vegetated cover was expanded by 24,530 ha (2.9%) while the non-vegetated cover was increased by 85,061 ha (10.2%) from 2020 to 2024. The major vegetation cover change was detected between 2010 and 2020 over the study area. Therefore, the change detection analysis of the results demonstrated that vegetation cover over the past 35 years was least expanded.

Table 4. *Change detection of vegetation cover change area in hectares.*

LCC	1990-2000	2000-2010	2010-2020	2020-2024	2010-2024	1990-2020	1990-2024	2000-2020
NV to NV	572,626	559,878	555,795	550,327	591,430	558,429	605,244	504,254
NV to V	150,491	26,111	113,7045	24,530	78,078	166,598	119,792	81,723
V to NV	13,363	107,769	190,755	85,061	43,980	16,438	30,168	69,432
V to V	95,933	138,660	146,096	174,742	121,188	93,201	79,470	177,000

Where NV= Non-vegetation, V=Vegetation and LCC=Land Cover Change
Source: Computed from Landsat image

3.4. Accuracy Assessment

The vegetation cover change accuracy assessment, including the Kappa coefficient, user accuracy, producer accuracy, and overall accuracy, is presented in Table 5. This assessment result showed that it was consistently high image classification confirmed [40]. Based on the result, both the user and producer accuracy image classifications for both class ranges were strictly high, ranging from 84.0% to 88.0% and 84.4% to 87.7%, respectively and both years. According to the accuracy assessment result, overall accuracy and kappa statistics were 85.3% and 70% in 2020, respectively. The overall accuracy and kappa coefficient of 2024 were 86.7% and 74%, respectively.

Table 5. *Accuracy assessments for the year 2020 and 2024.*

	2020		2024	
	vegetation	Non-veg.	vegetation	Non-veg.
User accuracy (%)	84.0	86.7	85.3	88.0
Producer accuracy (%)	86.3	84.4	87.7	85.7
Overall accuracy (%)	85.3		86.7	
Kappa statistics (%)	70		74	

Source: computed and taken 75 points from Google earth image for each years

3.5. Time Series and Trend Lines of Minimum, Maximum and Mean Rainfall

According to the result of the trend line, it showed that in (Figures 4, 5 and 6) the minimum, maximum, and mean rainfalls were decreasing from 1990–2024 over the study area. The trend line shows a slight decrease in mean rainfall of 0.26 mm per year over the 35-year period (1990-2024). This shows significant year-to-year fluctuations and a high rainfall variable in this region. The minimum rainfall trend line shows a decrease of 0.497 mm per year over the past 35-year period (1990-2024). This indicates approximately 17.4 mm of total minimum rainfall decrease and a dry trend in dry condition. The maximum rainfall also shows a decrease trend line of 0.81 mm per year. This suggests less extreme heavy rainfall events. The negative slope values show gradual decreases in minimum, maximum and mean rainfall. This happened a consistent downward trend, and the entire rainfall distribution was shifting towards a drier condition.

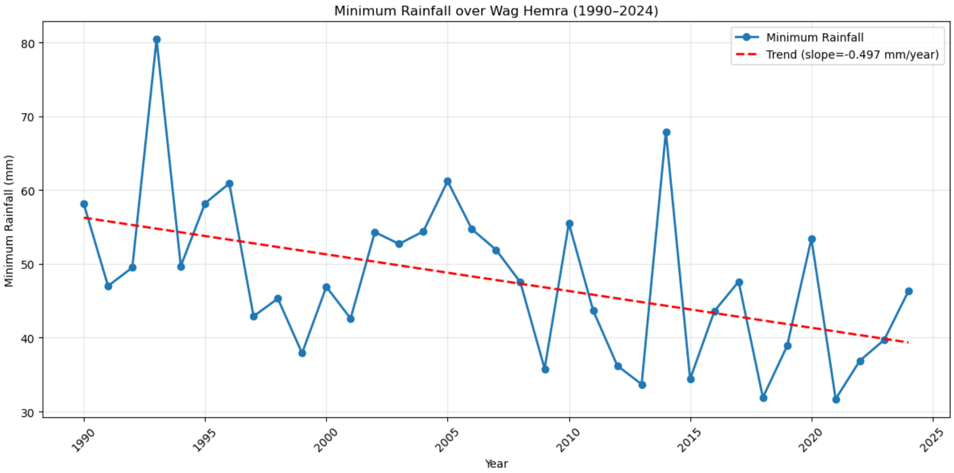

Figure 4. *Time series and trend line of minimum rainfall.*

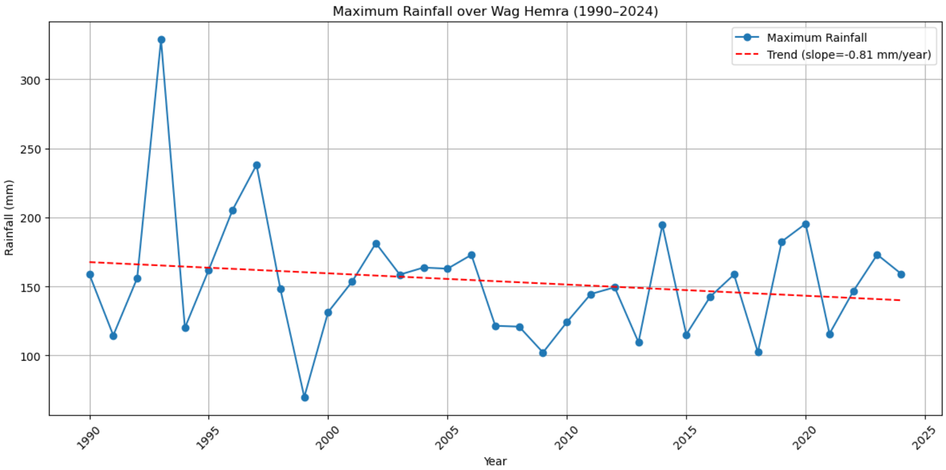

Figure 5. *Time series and trend line of maximum rainfall.*

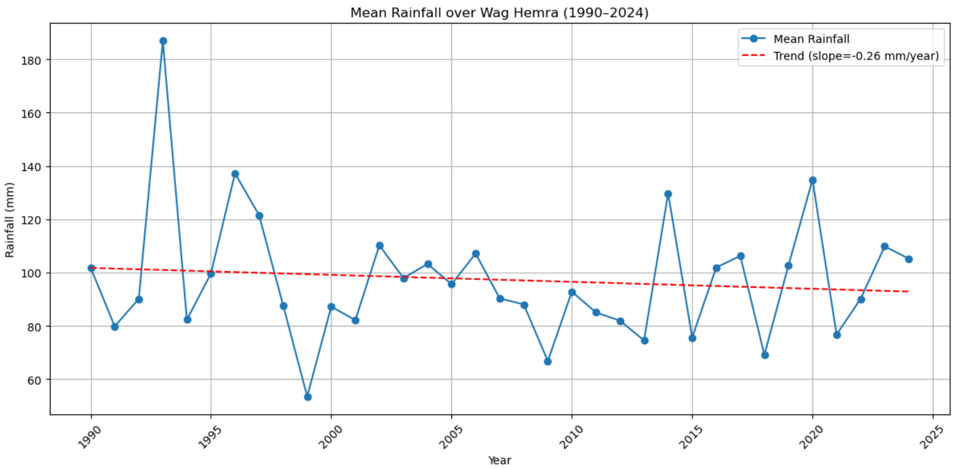

Figure 6. *Time series and trend line of mean rainfall.*

Ho: there is no trend in the time series analysis of the 35-year minimum, maximum, and mean rainfall.
Ha: there is a trend in the time series analysis of the 35-year minimum, maximum, and mean rainfall.

The calculated p-value is more significant than the significant level alpha = 0.05 since it prevents the null hypothesis Ho from being rejected. The probability of having to reject the null hypothesis Ho while it is true is 0.9%, 73%, and 89% for the minimum, maximum, and mean rainfall (Table 6). The maximum and mean rainfalls were not statistically significant as p-values of 0.73 and 0.89 are greater than alpha values of 0.05, respectively while the minimum rainfall was significant trend at p-value 0.009. The minimum, maximum and mean rainfall showed a decreasing trend with Kendall's tau values of -0.31, -0.04 and -0.02, respectively. According to the Mann-Kendall test result, the slope of minimum, maximum and mean rainfalls was changed by -0.47 mm, -0.28 mm and -0.04 mm per year respectively.

Table 6. *Mann-Kendall trend test of minimum, maximum and mean rainfalls.*

Variables	Minimum	Maximum	Mean
Observations	35	35	35
Kendall's tau	-0.31	-0.04	-0.02
Sen's slope	-0.47	-0.28	-0.04
p-value (Two-tailed)	0.009	0.73	0.89
Alpha	0.05	0.05	0.05

Source: Computed from Climate Hazard Center

3.6. The Changes of Vegetation Cover Impact on Rainfall

Areas with higher vegetation cover have shown considerable higher mean rainfall in the study area during the study period, whereas areas with low vegetation cover have shown low mean rainfall (Table 7). The present study is similar to a study by [41]; their finding is that a higher vegetation cover is found to increase rainfall in the Sahel. The statistical results revealed that all the minimum, maximum and mean rainfall of vegetation cover areas was greater than the non-vegetated areas in 1990. The mean rainfalls in both the vegetated and non-vegetated areas were 131.4 mm and 98.9 mm in 1990, respectively. The mean rainfalls in vegetated and non-vegetated areas were 95.1 mm and 85.8 mm in 2000, respectively. During the year 2010, the mean rainfall of the vegetation and non-vegetation areas increased to 101.4 mm and 92.3 mm, respectively. The mean rainfalls of vegetated and non-vegetated areas in 2020 were 151.1 mm and 131.1 mm, respectively. Hence, the mean rainfalls of both vegetated and non-vegetated areas in 2024 were 117.1 mm and 104.2 mm respectively.

Based on the analysis, the highest mean rainfall was revealed in 2020 with an amount of 195.4 mm, and the highest vegetation cover was seen in 2000, while the lowest mean rainfall was observed in 2010. The minimum, maximum, and mean rainfalls of the vegetation cover in 2000 were 57.0 mm, 126.6 mm, and 95.1 mm, respectively. The minimum, maximum, and mean rainfalls of the vegetated area in 2010 were 60.5 mm, 124.1 mm, and 101.4 mm respectively. Therefore, the result of the study revealed that vegetation cover has a positive effect on local rainfall.

Table 7. *Vegetation and non-vegetation areas with minimum, maximum and mean rainfall.*

Year		Land cover (ha)	Minimum	Maximum	Mean
1990	vegetated	112,280	105.3	158.7	131.4
	Non-vegetated	722,480	60.5	157.9	98.9
2000	vegetated	248,560	57.0	126.6	95.1
	Non-vegetated	586,202	50.0	131.4	85.8
2010	vegetated	168,321	60.5	124.1	101.4
	Non-vegetated	666,441	55.5	125.3	92.3
2020	vegetated	261,268	77.8	195.4	151.1
	Non-vegetated	573,494	64.6	194.6	131.1
2024	Vegetated	201,552	49.8	159.0	117.1
	Non-vegetated	633,210	47.9	159.0	104.2

Source: computed from Landsat and CHRIPS Satellite data

According to the analysis result, both trends of vegetation cover and mean rainfall were shown inclined from 1990 to 2024. From the graph, the lowest and highest vegetation covers were exhibited in 1990 and 2020 respectively. On the other hand, the lowest and highest mean rainfall were in 2000 and 2020 respectively over the study period. Therefore, the trend result (Figure 7) revealed that both vegetation cover and mean rainfall had a strong positive relationship during the study period.

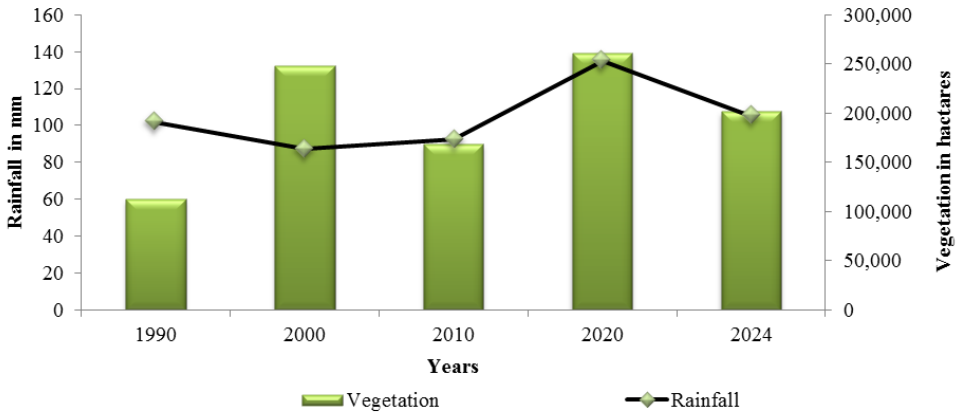

Figure 7. *Vegetation covers (ha) with mean rainfall (mm); computed from Landsat and CHRIPS satellite data.*

3.7. The Relationship of NDVI with Rainfall

There was a substantial positive linear association between mean NDVI and mean rainfall; however, the Pearson correlation data analysis showed that there was a statistically significant connection between the vegetation index of the mean NDVI and the mean rainfall, as the p-value of 0.00023 is smaller than the significant level of alpha value of 0.05. The correlation coefficient R between the mean NDVI and the mean rainfall was 0.17 (Table 8). Therefore, the analysis of the Pearson correlation result showed that the mean rainfall had a positive correlation with the mean NDVI (Table 8). This result is consistent with [42]. They did their study on the effects of tropical vegetation on rainfall. Their result reported that changes in the surface vegetation cover can alter local rainfall. The result of the present study is also in agreement with the study by [26], whose finding proposed that the tropical savannah correlates 62.44% of the vegetation cover positively with rainfall in climate zones of Africa.

Table 8. *NDVI in relation to rainfall.*

variables	Mean NDVI with mean rainfall
p-value	0.00023
Alpha value	0.05
R	0.17
R^2	0.03

Source: computed from Landsat and CHRIPS image

The coefficient of determination R^2 revealed that 3% of rainfall change is caused by vegetation cover change in the study area, which means that vegetation cover has a positive impact on rainfall. This study is consistent with [11] report that 23% of rainfall change is due to the change in vegetation cover in the central, northern, and southeastern parts of the study area in Ethiopia. This analysis result suggested that, in the eastern, north-eastern, and south-eastern regions of the research study, an area with considerable NDVI and rainfall value has been discovered in Figure 8. The findings demonstrate that during the study period, areas with low NDVI values had considerably little rainfall, whereas those with high NDVI values demonstrated considerably moderate amounts of rainfall. This study is similar to the [14, 43].

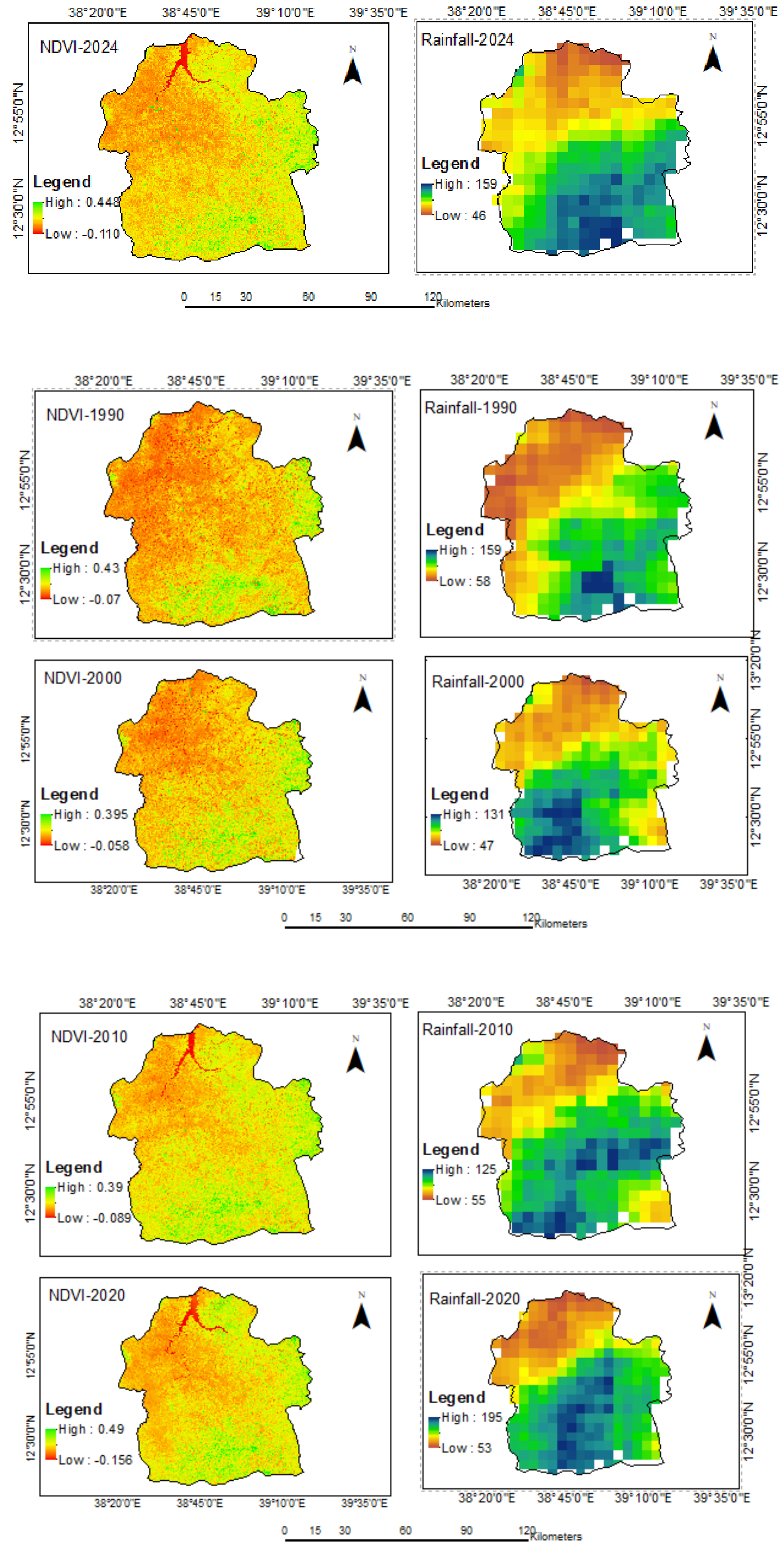

Figure 8. *The relationship of NDVI and rainfall, sources: computed from Landsat and chirps satellite dataset.*

4. Conclusion

Landsat imagery has the ability to assess the effect of vegetation cover change on rainfall. This study uses NDVI values as a proxy for observing vegetation cover in the southern and southeastern parts of the Wag Hemra Zone, Ethiopia. The mean NDVI values of all reference years were below 0.1, which means the average vegetation cover was poor in the study area (1990-2024). Threshold results indicated that 13.5% of the study area was covered by vegetation in 1990, which had increased to 29.8% by 2000, and also decreased to 20.2% by 2010. Based on the analysis of the NDVI results, the vegetation cover in 2020 accounted for 31.3% and was the highest percentage of vegetation cover in the study area, which had also decreased to 24.1% by 2024. Over the past thirty-five years, based on the vegetation cover analysis, the amount of vegetation covered from 1990 to 2024 increased by 89,272 ha. This indicated that there was least increased the area of vegetation cover in the study area. Using image differencing, there was the largest vegetation restored area of 166,598 ha from 1990 to 2020 and the smallest vegetation cover changed area of 13,363 ha within a reference year from 1990 to 2000. Change detection analysis of image differentiation revealed that the highest vegetation removed from the area (from vegetated to non-vegetated) from 2010 to 2020 was shown 190,755 ha (22.9%). Therefore, the change detection analysis of the results demonstrated that vegetation cover over the past 35 years was least expanded than degraded. The vegetation cover change accuracy assessment was consistently high, as confirmed by the image classification. The minimum, maximum, and mean rainfalls were decreasing trend lines of 0.497, 0.81 and 0.26mm per year over the past 35 years period (1990-2024) respectively. This negative slope values show gradual decreases in rainfall and consistent downward trends. The maximum and mean rainfalls were not statistically significant as p-values of 0.73, and 0.89 but the minimum rainfall were a statistically significant trend at p-value 0.009. The minimum, maximum and mean rainfall showed a decreasing trend with Kendall's tau values of -0.31, -0.04 and -0.02, respectively. The mean rainfall of vegetated area was greater than the mean rainfall of non-vegetated area for all reference years. This indicates areas with low vegetation cover have shown low mean rainfall. The analysis of the Pearson correlation result showed that the mean rainfall had a positive correlation with the mean NDVI. Based on the coefficient of determination, 3% of vegetation cover change was caused by rainfall in the study area. This indicates areas with low NDVI values had considerably little rainfall and vice versa. Therefore, the result of the study revealed that vegetation cover has a positive effect on local rainfall. Generally, all the residents of Wag Hemra zone are to strengthen the protection of the vegetation cover in the study area, encourage afforestation work, and stakeholders should cooperate and integrate their plans and work on a natural resource conservation plan to do a fruitful job.

Abbreviations

CHRIPS	Climate Hazards Group Infrared Precipitation with Stations
NDVI	Normalized Difference Vegetation Index
USGS	United States Geological Survey
OLI	Operational Land Imager
TM	Thematic Mapper
TIRS	Thermal Infra-Red
ENVI	Environment for Visualizing Images
MK	Mann-Kendall
LCC	Land Cover Change

Acknowledgments

First, I thank God for keeping me healthy and for adding the performance of my study. I would like to thank the Ethiopian Meteorology Institute for providing the raw meteorological data. Also I am grateful to the colleagues of the East Amhara Meteorology Service Center.

Author Contributions

Wendimnew Getachew Alemu is the sole author. The author read and approved the final manuscript.

Funding

This research has never been any funded.

Conflicts of Interest

I declare no conflicts of interest.

References

[1] R. Almalki, M. Khaki, P. M. Saco, and J. F. Rodriguez, "Monitoring and Mapping Vegetation Cover Changes in Arid and Semi-Arid Areas Using Remote Sensing Technology: A Review," *Remote Sens.*, vol. 14, no. 20, 2022, https://doi.org/10.3390/rs14205143

[2] S. Islam, T. Yeasmin, and S. Karmaker, "Vegetation Cover Change Analysis during 1989-2020 of Coastal Barguna District, Bangladesh Using Remote Sensing and GIS Technology," vol. 11, no. 2, pp. 259–277, 2023.

[3] M. Ibrahim and A. Al-Mashagbah, "Change Detection of Vegetation Cover Using Remote Sensing Data as a Case Study: Ajloun Area," *Civ. Environ. Res.*, vol. 8, no. 5, pp. 1–5, 2016.

[4] T. Geremew and H. Jebessa, "Climate change and its effects on vegetation phenology across ecoregions of Ethiopia," vol. 13, 2017.

[5] I. Ali, Z. Muhammad, and H. Khan, "Impact of climate change on spatiotemporal variations in the vegetation cover and hydrology of district Nowshera," vol. 13, no. 11, pp. 3867–3882, 2022, https://doi.org/10.2166/wcc.2022.229

[6] K. Mangwale, C. M. Shackleton, and A. Sigwela, "Changes in forest cover and carbon stocks of the coastal scarp forests of the Wild Coast, South Africa," vol. 2620, no. February, 2017, https://doi.org/10.2989/20702620.2016.1255480

[7] S. Suresh and K. Mani, "Application of remote sensing in understanding the relationship between ndvi and lst," vol. 138527, pp. 99–105, 2017.

[8] F. T. Gelata, "Application of GIS using NDVI and LST estimation to measure climate variability-induced drought risk assessment in Ethiopia," vol. 14, no. 7, pp. 2479–2489, 2023, https://doi.org/10.2166/wcc.2023.154

[9] J. Gamon, S. Peng, and A. Chen, "Using Remote Sensing and GIS in Measuring Vegetation Cover Change from Satellite Imagery in Mosul City, North of Iraq Using Remote Sensing and GIS in Measuring Vegetation Cover Change from Satellite Imagery in Mosul City, North of Iraq," 2020, https://doi.org/10.1088/1757-899X/757/1/012062

[10] P. P. Gogoi, V. Vinoj, D. S, G. Roberts, J. Dash, and S. Tripathy, "Land use and land cover change effect on surface temperature over Eastern India," no. July 2018, pp. 1–10, 2019, https://doi.org/10.1038/s41598-019-45213-z

[11] W. Nega, B. Tesfaw, and A. Fetene, "Remote Sensing Applications : Society and Environment An assessment of the vegetation cover change impact on rainfall and land surface temperature using remote sensing in a subtropical climate, Ethiopia," *Remote Sens. Appl. Soc. Environ.*, vol. 16, no. May, p. 100266, 2019, https://doi.org/10.1016/j.rsase.2019.100266

[12] B. Baniya, Q. Tang, Z. Huang, S. Sun, and K. anan Techato, "Spatial and temporal variation of NDVI in response to climate change and the implication for carbon dynamics in Nepal," *Forests*, vol. 9, no. 6, pp. 1–18, 2018, https://doi.org/10.3390/f9060329

[13] C. Study, "Land surface temperature changes caused by land cover/ land use properties and their impact on rainfall characteristics," vol. 9, no. 3, pp. 353–372, 2023, https://doi.org/10.22035/gjesm.2023.03.01

[14] N. Joshi, P. Gyawali, S. Sapkota, D. Neupane, S. Shrestha, and N. Shrestha, "Analyzing the effect of climate change (rainfall and temperature) on vegetation cover of nepal using time series," vol. iv, no. june, pp. 10–14, 2019.

[15] S. Zerkani, E. H. Abba, H. Zerkan, T. Zair, and N. E. Zine, "The impact of the precipitation on the vegetation and ecological quality in the River of Oued Guigou, Morocco," *IOP Conf. Ser. Earth Environ. Sci.*, vol. 1090, no. 1, 2022, https://doi.org/10.1088/1755-1315/1090/1/012036

[16] Y. Wang, D. Peng, M. Shen, X. Xu, and X. Yang, "Contrasting Effects of Temperature and Precipitation on Vegetation Greenness along Elevation Gradients of the Tibetan Plateau," 2020.

[17] S. Batool, K. Khan, A. Ghaffar, and S. Z. Hussain, "Forest cover change detection and its impact on rainfall patternin thak valley (pakistan)," 2015.

[18] A. Mani φba *et al.*, "Using Remote Sensing to Quantify the Joint Effects of Climate and Land Use / Land Cover Changes on the Caatinga Biome of Northeast Brazilian," pp. 1–27, 2022.

[19] F. Gurmessa, "Forest loss and climate change in Ethiopia," *Res. J. Agric. Environ. Manag.*, vol. 4, no. 5, pp. 216–224, 2015.

[20] V. Agone, "Change detection of vegetation cover Using Remote Sensing and GIS," no. April 2012, 2019.

[21] S. S. Rwanga and J. M. Ndambuki, "Accuracy Assessment of Land Use/Land Cover Classification Using Remote Sensing and GIS," *Int. J. Geosci.*, vol. 08, no. 04, pp. 611–622, 2017, https://doi.org/10.4236/ijg.2017.84033

[22] C. Funk *et al.*, "The climate hazards infrared precipitation with stations - A new environmental record for monitoring extremes," *Sci. Data*, vol. 2, pp. 1–21, 2015, https://doi.org/10.1038/sdata.2015.66

[23] L. Harrison *et al.*, "Advancing early warning capabilities with CHIRPS-compatible NCEP GEFS precipitation forecasts," *Sci. Data*, vol. 9, no. 1, pp. 1–13, 2022, https://doi.org/10.1038/s41597-022-01468-2

[24] B. Nile and Y. Bayissa, "Evaluation of Satellite-Based Rainfall Estimates and Application to Monitor Meteorological Drought for," pp. 1–17, 2017, https://doi.org/10.3390/rs9070669

[25] C. Toté, D. Patricio, H. Boogaard, R. Van Der Wijngaart, E. Tarnavsky, and C. Funk, "Evaluation of Satellite Rainfall Estimates for Drought and Flood Monitoring in Mozambique," pp. 1758–1776, 2015, https://doi.org/10.3390/rs70201758

[26] V. Nzabarinda, A. Bao, W. Xu, and S. Uwamahoro, "A Spatial and Temporal Assessment of Vegetation Greening and Precipitation Changes for Monitoring Vegetation Dynamics in Climate Zones over Africa," 2021.

[27] S. Hussain *et al.*, "Relation of land surface temperature with different vegetation indices using multi ‑ temporal remote sensing data in Sahiwal region, Pakistan," *Geosci. Lett.*, 2023, https://doi.org/10.1186/s40562-023-00287-6

[28] S. Hussain and S. Karuppannan, "Land use/land cover changes and their impact on land surface temperature using remote sensing technique in district Khanewal, Punjab Pakistan," *Geol. Ecol. Landscapes*, vol. 00, no. 00, pp. 1–13, 2021, https://doi.org/10.1080/24749508.2021.1923272

[29] O. Ibrahim, A. Balasmeh, and T. Karmaker, "Effect of Temperature and Precipitation on the Vegetation Dynamics of High and Moderate Altitude Natural Forests in India Effect of Temperature and Precipitation on the Vegetation Dynamics of High and Moderate Altitude Natural Forests in India," *J. Indian Soc. Remote Sens.*, no. December, 2019, https://doi.org/10.1007/s12524-019-01065-8

[30] G. M. Gandhi, S. Parthiban, N. Thummalu, and A. Christy, "Ndvi: Vegetation Change Detection Using Remote Sensing and Gis - A Case Study of Vellore District," *Procedia Comput. Sci.*, vol. 57, p. 2015, https://doi.org/10.1016/j.procs.2015.07.415

[31] M. D. K. L. Gunathilaka and S. L. J. Fernando, "Accuracy Assessment of Unsupervised Land Use and Land Cover Classification Using Remote Sensing and Geographical Information Systems," *Int. J. Environ. Eng. Educ.*, vol. 4, no. 3, pp. 76–82, 2022, https://doi.org/10.55151/ijeedu.v4i3.73

[32] S. Shrestha, K. N. Poudyal, N. Bhattarai, M. B. Dangi, and J. J. Boland, "An Assessment of the Impact of Land Use and Land Cover Change on the Degradation of Ecosystem Service Values in Kathmandu Valley Using Remote Sensing and GIS," *Sustain.*, vol. 14, no. 23, 2022, https://doi.org/10.3390/su142315739

[33] S. Vijitharan, N. Sasaki, M. Venkatappa, N. K. Tripathi, I. Abe, and T. W. Tsusaka, "Assessment of Forest Cover Changes in Vavuniya District, Sri Lanka : Implications for the Establishment of Subnational Forest Reference Emission Level," 2022.

[34] V. K. A. Somayajula *et al.*, Classification and Validation of Spatio-Temporal Changes in Land Use/Land Cover and Land Surface Temperature of Multitemporal Images, vol. 14, no. 23. 2022. https://doi.org/10.3390/su142315677

[35] F. T. Gelata, H. Jiqin, and S. Chaka Gemeda, "Application of MK trend and test of Sen's slope estimator to measure impact of climate change on the adoption of conservation agriculture in Ethiopia," *J. Water Clim. Chang.*, vol. 14, no. 3, pp. 977–988, 2023, https://doi.org/10.2166/wcc.2023.508

[36] A. Gadedjisso-tossou and K. I. I. Adjegan, "Rainfall and Temperature Trend Analysis by Mann – Kendall Test and Significance for Rainfed Cereal Yields in," pp. 1–20, 2021.

[37] A. Panda and N. Sahu, "Trend analysis of seasonal rainfall and temperature pattern in Kalahandi, Bolangir and Koraput districts of Odisha, India," *Atmos. Sci. Lett.*, vol. 20, no. 10, pp. 1–10, 2019, https://doi.org/10.1002/asl.932

[38] P. Schober and C. Boer, "Correlation Coefficients: Appropriate Use and Interpretation," no. August, 2018, https://doi.org/10.1213/ANE.0000000000002864

[39] K. S. Meshesha, "Evaluating the relationship of vegetation dynamics with Rainfall and Land Surface Temperature using geospatial techniques in South Wollo zone, Ethiopia," pp. 1–28, 2023.

[40] O. A. Isioye, E. A. Akomolafe, U. H. Ikwueze, S. Indices, and G. C. Index, "Accuracy analysis of sentinel 2a and landsat 8 oli + satellite datasets over kano state (nigeria) using vegetation spectral indices," vol. xliv, no. december, pp. 65–72, 2020.

[41] C. Dyn, "The effect of vegetation changes on precipitation and Mesoscale Convective Systems in the Sahel The effect of vegetation changes on precipitation and Mesoscale Convective Systems in the Sahel," no. September, 2009, https://doi.org/10.1007/s00382-009-0539-2

[42] J. H. Marsham, "The Effects of Tropical Vegetation on Rainfall," 2018.

[43] H. Khalis *et al.*, "Effects of climate change on vegetation cover in the oued lahdar watershed. Northeastern Morocco," *Plants*, vol. 10, no. 8, pp. 1–16, 2021, https://doi.org/10.3390/plants10081624